Desalination and Water Treatment
www.deswater.com

doi: 10.1080/19443994.2015.1007088

57 (2016) 5673–5685
March

Taylor & Francis
Taylor & Francis Group

Artocarpus camansi Blanco (Breadnut) core as low-cost adsorbent for the removal of methylene blue: equilibrium, thermodynamics, and kinetics studies

Linda B.L. Lim[a,*], Namal Priyantha[b,c], Hei Ing Chieng[a], Muhammad Khairud Dahri[a]

[a]*Faculty of Science, Department of Chemistry, Universiti Brunei Darussalam, Jalan Tungku Link, Gadong, Brunei Darussalam, Tel. +673 8748010; Fax: +673 2461502; email: linda.lim@ubd.edu.bn (L.B.L. Lim), Tel. +673 8717770; email: huiing.250@gmail.com (H.I. Chieng), Tel. +673 8875789; email: kiddri86@hotmail.com (M.K. Dahri)*
[b]*Faculty of Science, Department of Chemistry, University of Peradeniya, Peradeniya, Sri Lanka, Tel. +94 0718672632; email: namalpriyantha@pdn.ac.lk*
[c]*Postgraduate Institute of Science, University of Peradeniya, Peradeniya, Sri Lanka*

Received 31 May 2014; Accepted 26 December 2014

ABSTRACT

This study investigates the adsorption characteristics of methylene blue (MB) on core of breadnut, *Artocarpus camansi* Blanco. Oven-dried *Artocarpus camansi* core (ACC), with point of zero charge at pH 4.1, was found to be very effective in removing MB when compared to most literature reported fruit biomasses. Six isotherm models coupled with error analyses were used to investigate possible models of adsorption. Both the Langmuir and Sips models were found to give the best fit with maximum adsorption capacity, measured as mg of MB per g of adsorbent, of 369 and 328 mg g^{-1}, respectively. Thermodynamics studies showed that the adsorption process was both spontaneous and exothermic. Fast kinetics, with 50% MB being removed within 5 min when 50 mg L^{-1} dye solution was used, showed pseudo-second-order. Fourier transform infrared, X-ray fluorescence, and scanning electron microscopic investigation of ACC before and after MB adsorption conclusively demonstrated that oven-dried breadnut core has great potential to be used as a low-cost adsorbent for the removal of MB.

Keywords: Breadnut core; Biomass; Methylene blue; Adsorption; Kinetics; Cationic dye

1. Introduction

With the world population now at over 7 billion and still growing, there is an increasing demand in safe drinking water and freshwater for both public health and development. Water is a finite natural resource and its high consumption by the growing population, therefore, poses a serious problem. Increase in industrialization to cater to the population growth results in the discharge of industrial effluents causing water to be polluted. One of the serious problems of wastewaters is due to dye effluents being discharged into the water system. Even at very low concentrations, these dyes are visible due to their high extinction coefficients. Being highly resistant to fading as well as having toxic effects, these highly colored effluents not only impede light penetration but also destroy aquatic communities, thereby disrupting the biological processes within the water system.

Treatment of wastewater is therefore becoming increasingly important and various methods have

*Corresponding author.

been developed to remove dye pollutants from industrial effluents [1]. One such method which has gained popularity due to its high efficiency in removing dyes is the use of activated carbon in adsorption technology. However, as commercial activated carbon is expensive, attention has now been focused on the use of low-cost adsorbents as alternatives. To date, many different adsorbents have been reported [2–4].

This paper focuses on a new low-cost adsorbent, *Artocarpus camansi* Blanco, from the *Artocarpus* genus of the *Moraceae* family. It is commonly known as breadnut and the locals in Brunei Darussalam call it "Kemangsi". Unlike the more popular jackfruit (*Artocarpus heterophyllus*) and breadfruit (*Artocarpus altilis*), breadnut is less commonly found in Brunei Darussalam. The fruits are usually smaller in size and the seeds are eaten either as a vegetable dish, or boiled, or roasted as nuts. The peel and core of *Artocarpus* fruits, which could make up to >70% of the fruit [5,6], are the inedible parts of the fruit with no economical value and are discarded as waste. There have not been many reports on the use of *Artocarpus* as low-cost adsorbent. It has already been reported that jackfruit peel can be used to remove dyes [7–10] and heavy metal ions [11], and jackfruit leaf [12,13] for the removal of dyes. Our recent investigation showed that the core of tarap (*Artocarpus odoratissimus*) and breadfruit (*Artocarpus altilis*) was able to remove Cd(II) and Cu(II) [14,15] while the peel of tarap [16], breadfruit [17] and breadnut (*Artocarpus camansi*) [18,19] were successfully used as adsorbents for the removal of dyes.

In this study, the aim was to investigate the use of *Artocarpus camansi* core (ACC) as a new potential low-cost adsorbent for the removal of the cationic dye, methylene blue, (MB) from aqueous solution. Characterization of the adsorbent was performed by elemental analysis for C, H, N, and S, Fourier transform infrared spectroscopy (FTIR), point of zero charge (pH_{pzc}) measurements, scanning electron microscopy (SEM), and X-ray fluorescence (XRF) spectroscopy. The effects of shaking time, settling time, medium pH, and ionic strength on the extent of adsorption, and thermodynamics and kinetics of adsorption of ACC with MB were also investigated.

2. Experimental

2.1. Materials

The *Artocarpus camansi* fruits were purchased by selecting them randomly from the local open markets in the Brunei-Muara District of Brunei Darussalam. The core was separated from the rest of the fruit and oven dried at 80°C to obtain a constant mass. This temperature was specifically selected to remove moisture without decomposing the organic matter present in the adsorbent. No other pre-treatment of samples by either physical or chemical means prior to adsorption studies was carried out. The dried sample was blended, sieved, and thoroughly mixed to ensure uniformity prior to using them. The fraction of ACC with particle size between 355 and 850 μm was used for all experiments in this study. Higher particle sizes are less efficient for dye removal, while smaller sizes are not desirable for expansion of this work for large volumes. All experiments were carried out in duplicate/triplicate at 24°C with ACC-MB (solid-solution) ratio of 1:500, unless otherwise stated.

2.2. Characterization of ACC

A dried ACC sample was analyzed for its fat, fiber, and protein contents using GerhardT Soxtherm multistate/SX PC, GerhardT Fibretherm FT12, and GerhardT VAP 50S Nitrogen Protein Analyzer, respectively. XRF PANalytical Axios^{max} was used to characterize the elements present in ACC. Tescan Vega XMU SEM was used for morphological characteristics of the adsorbent surface which was coated with SPI-MODULE™ Sputter Coater. KNO_3 solution of 0.10 M with pH adjustment to the required value (2, 4, 6, 10, and 12) by the addition of 0.1 M HNO_3 and 0.1 M NaOH was used for the determination of the pH_{pzc}. In this experiment, KNO_3 solution (25.0 mL) at different pHs was added into separate flasks each filled with pre-weighed ACC (0.050 g) and agitated on an orbital shaker at 250 rpm for 2 h. Functional groups present in ACC were analyzed using FTIR spectrophotometer (Shimadzu Model IRPrestige-21). The contents C, H, N, and S were analyzed in the Elemental Analysis Laboratory at the National University Singapore. UV–vis spectrophotometer (Shimadzu/Model UV-1601PC) was used to measure the absorbance of MB at the wavelength set at λ_{max} = 664.0 nm, in all experiments for the determination of the concentration of MB in solution.

2.3. Chemicals and reagents

A 1,000 mg L^{-1} MB stock solution, prepared by dissolving MB in distilled water, was used to prepare a series of MB concentrations ranging from 10 to 1,000 mg L^{-1}. MB was purchased from Sigma-Aldrich Corporation, solution of different pH solutions, which was prepared using NaOH and HNO_3, both of which were purchased from Fluka. All chemicals were used without further purification.

2.4. Optimization of parameters

2.4.1. Effect of contact time

The effects of contact (shaking and settling) time were determined by shaking a mixture of ACC in 10.0 mg L^{-1} MB dye solution (ratio ACC:solution = 1:500) at 250 rpm at ambient temperature for different shaking times ranging from 30 to 240 min. Each solution was filtered through a fine metal sieve after shaking and the absorbance of the filtrate was determined for the remaining MB dye content. The ACC-MB dye mixture was allowed to settle for different time periods up to 240 min to ensure that total equilibrium has reached. The filtrate was analyzed as previously stated.

2.4.2. Effect of pH

To investigate the effect of medium pH, the sample in each dye solution (10 mg L^{-1}) was adjusted to pH ranging from 2 to 10 and shaken for the optimized shaking time and settling time. Each solution was then filtered and the filtrate was analyzed.

2.4.3. Effect of ionic strength

ACC (0.050 g) was added to 100 mg L^{-1} MB solution and diluted using KNO_3 and KCl solution of concentration ranging from 0.01 to 1.0 M. The solutions were shaken to the optimum shaking and settling times. The ACC-MB dye mixture was separated and the filtrate was analyzed.

2.5. Thermodynamics studies

ACC (0.050 g) was mixed with 100 mg L^{-1} MB dye solution (25.0 mL) and shaken using water bath shaker with temperature adjusted to 24, 40, 50, 60, and 70°C (298, 314, 324, 334, and 344 K) for pre-determined shaking time and allowed for pre-determined settling times. The solution was then filtered and the filtrate was analyzed. Thermodynamics parameters such as Gibbs free energy (ΔG°), enthalpy (ΔH°), and entropy (ΔS°) were subsequently calculated.

2.6. Adsorption isotherms

ACC samples were separately treated with a series of MB solutions of concentrations ranging from 0 to 1,000 mg L^{-1} and treated for the optimum shaking and settling time periods. The solution was filtered and the filtrate was analyzed.

2.7. Kinetics adsorption of MB on ACC

Each adsorbent sample (0.050 g) was mixed with 10.0 mg L^{-1} of MB solution (25.0 mL), and the suspension was stirred as soon as mixing commenced. Samples were withdrawn at every one minute intervals until the equilibrium was reached. Each solution was filtered and the filtrate was analyzed.

3. Results and Discussion

3.1. General Characterization of ACC sample

Elemental analysis showed that ACC contains 40.8% C, 5.5% H, 2.7% N, and <1.0% S. Analysis of ACC for fat, fiber, and protein gave 3.5, 21.9, and 8.3%, respectively. Even though, in terms of appearance and texture, the peel and the core of *Artocarpus camansi* are very different with the core being more sponge-like, both gave similar results in elemental analysis and fat, fiber, and protein contents [18]. As fibers have been used as low-cost adsorbents [20–22], high fiber content in ACC could be an asset for adsorption of MB.

3.1.1. Analysis of elements by XRF

Characterization of ACC by XRF showed the presence of different elements, such as K, Ca, Zn, Si, and Fe (Table 1). Of these, K, Zn, and Ca were the three major elements present at 28.1, 14.2, and 12.2%, respectively. Fig. 1 shows that adsorption of MB on ACC significantly reduces K from 28.1 to 3.5%. Since the dye used is a cationic dye, there is a possibility that the cationic dye molecules replace metal ions such as K^+ with their partial hydration sphere, which could be present at a high concentration without having strong binding. The same effect was also reported in other *Artocarpus* species as well [16].

3.1.2. Point zero charge

The pH_{pzc} of ACC was determined from a plot of ΔpH_{pzc}, the difference between initial pH and final pH, against pH_i (initial pH). The point where there is no change in pH is pH_{pzc}. The pH_{pzc} of ACC, determined using 0.1 M KNO_3, was at approximately 4.1 suggesting that the surface of adsorbent would be predominantly positively charged at pH < 4.1 and negatively charged at pH > 4.1. The corresponding *Artocarpus camansi* peel has a slightly higher pH_{pzc} of 4.8 [18]. The pH_{pzc} of *Artocarpus odoratissimus* (tarap) core was reported to be at pH 9.2 [14], while that of the leaf of *Artocarpus heterophyllus* (jackfruit) was at pH 3.9 [13].

Table 1
Characterization of elements of ACC by XRF

Elements	Result (%)	Elements	Result (%)	Elements	Result (%)
O	25.5	S	1.2	Zn	14.2
Mg	1.9	Cl	4.2	Rb	0.1
Mn	0.1	K	28.1	Sr	0.1
Si	1.6	Ca	12.2	Ru	0.8
P	2.3	Fe	7.7	Ni	0.2

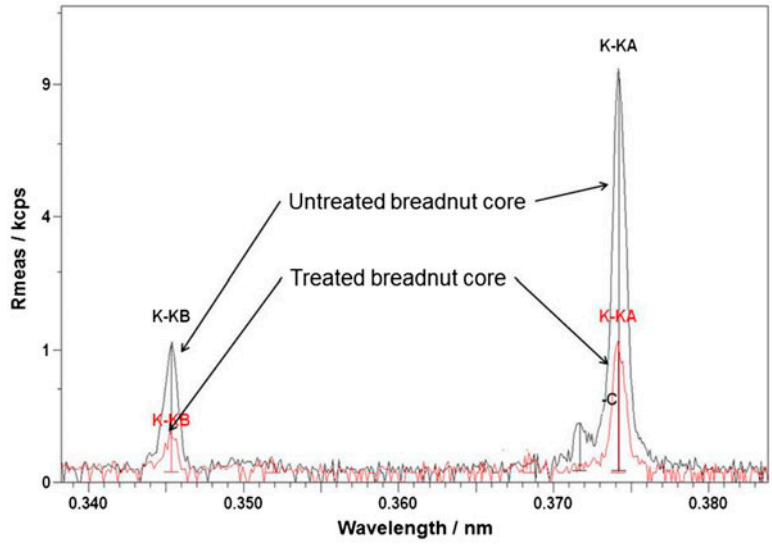

Fig. 1. XRF spectra showing element *K* of ACC before and after adsorption with MB.

3.1.3. SEM analysis of ACC

The surface morphology of ACC was analyzed using SEM. Before adsorption of MB shows that the surface of ACC contains many pores and cavities of irregular sizes (Fig. 2(i)). On treatment with MB, the surface morphology of ACC becomes less rough as a result of dye adsorption on the pores/cavities (Fig. 2(ii)).

3.2. Optimization of parameters

3.2.1. Effect of contact time

The effect of shaking time on the extent of removal of MB showed rapid removal of the dye at initial stages of contact with the system, reaching equilibrium within 180 min (Fig. 3(a)). Compared to the core, the peel of *Artocarpus camansi* required 60 min to reach equilibrium, while 240 and 120 min contact times were required for *Artocarpus odoratissimus* peel [16] and peat [3,23], respectively, under the same experiment conditions. When applied to wastewater treatment, fast uptake of adsorbate by an adsorbent is especially crucial which signifies that the adsorbent is efficient to be used in wastewater treatment.

Having determined the shaking time required, the next step was to investigate the effect of settling time. It was found that 60 min (Fig. 3(b)) was sufficient for the system to reach its total equilibrium. Hence, all subsequent experiments, unless otherwise stated, were carried out with 180 min shaking time followed by 60 min settling time.

3.2.2. Effect of medium pH

An important parameter in adsorption is the effect of pH in dye solution. The effect of pH on adsorption of MB on ACC was carried out from pH 2 to 10. At the ambient pH of MB (pH 6), 86% of MB was adsorbed by ACC under laboratory conditions (Fig. 4). As the pH decreases from 5 to 2, the amount of MB being adsorbed also decreases *i.e.* from 79% at pH 5 to 38% at pH 2. Similar effects were also reported for

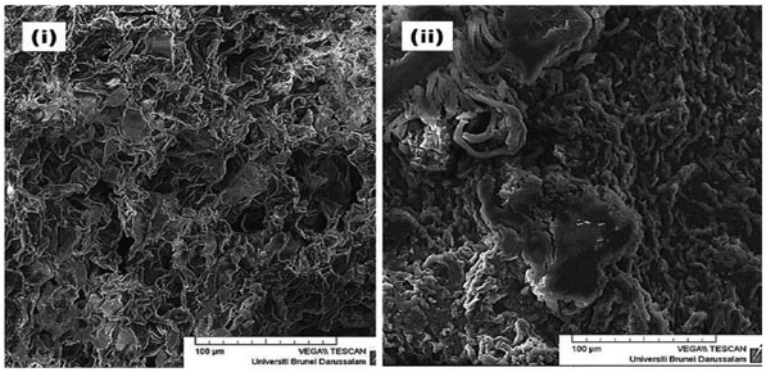

Fig. 2. SEM of ACC showing (i) before treatment (ii) after treatment with MB.

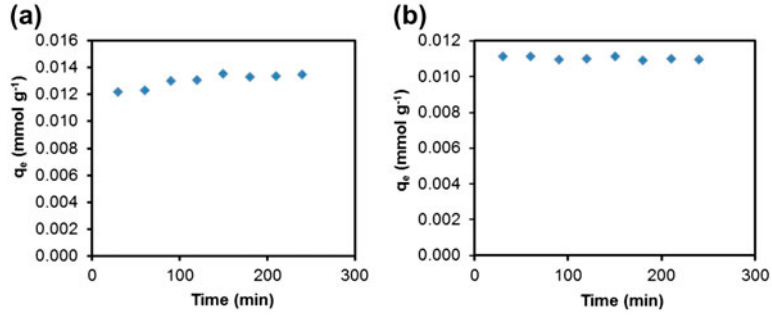

Fig. 3. Effect of (a) shaking time and (b) settling time on adsorption of MB on ACC (mass of ACC = 0.050 g; volume of MB solution = 25.0 mL; concentration of MB = 10.0 mg L^{-1}).

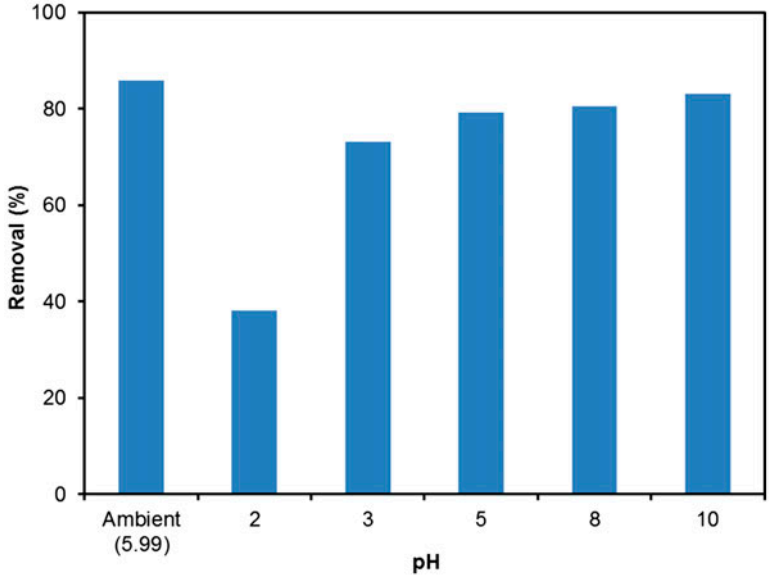

Fig. 4. The effect of medium pH on the removal of MB by ACC (mass of ACC = 0.050 g; volume of MB solution = 25.0 mL; concentration of MB = 10.0 mg L^{-1}).

jackfruit peel and leaf [8,13]. This could be due to the surface of the ACC being more positively charged at lower pH. MB, being a cationic dye, would have a greater electrostatic repulsion with the positively charged adsorbate, resulting in the drastic decrease in dye removal observed at pH 2 [24]. On the other hand, at ambient pH or pH > pH_{pzc}, the negatively charged surface of ACC favors adsorption of cationic MB. Since there was little effect on the amount of MB being adsorbed from ambient conditions to pH 10, the ambient pH was chosen for all the other experiments in this study.

3.2.3. Effect of ionic strength

Effect of ionic strength showed a general decrease in the removal of MB by ACC when the concentration of KNO_3 was increased (Fig. 5). As the concentration of KNO_3 increases from 0 to 0.001 M, only a slight decrease in the % removal was observed. However, from 0.001 to 0.01 M, a drastic reduction of approximately 50% was observed followed by a gradual decrease of about of 20% up to 0.8 M KNO_3. This indicates that the ionic strength of the medium has strong influence on the adsorption of MB on ACC. The reduction in the adsorption could be due to the electrostatic force of attraction between ACC and MB, further supporting the previous argument that there is a competition between the K^+ ions and MB for the limited number of sites available for sorption process [25,26]. It should be stated that there is no difference between KNO_3 and KCl in the investigation of the effect of ionic strength on adsorption of MB over the concentration range under investigation.

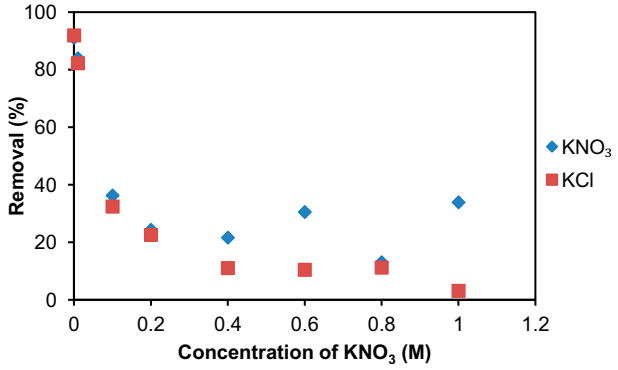

Fig. 5. The effect of ionic strength on the removal of MB (mass of ACC = 0.050 g; volume of MB solution = 25.0 mL; concentration of MB = 100.0 mg L^{-1}).

3.3. Thermodynamics parameters

Thermodynamics studies were carried out in order to understand the adsorption process of MB onto ACC. The Van't Hoff plot of ln K_c vs. $1/T$ gave linear regression $R^2 = 0.9855$. The changes in Gibbs free energy (ΔG°), enthalpy (ΔH°), and entropy (ΔS°) for the adsorption process were determined using Eqs. (1) and (2).

$$\Delta G^\circ = -RT\ ln\ K_c \tag{1}$$

where ΔG° is the Gibbs free energy (kJ mol^{-1}), R is the universal gas constant (8.314 J mol^{-1} K^{-1}), T is the absolute temperature (K) and K_c is the equilibrium constant (C_s/C_e). C_s is the concentration of dye on adsorbent (mg L^{-1}) and C_e is the equilibrium concentration of MB (mg L^{-1}). The enthalpy (ΔH°) and entropy (ΔS°) values can be calculated from the Van't Hoff equation [27]:

$$ln\ K_c = -\frac{\Delta H^\circ}{RT} + \frac{\Delta S^\circ}{R} \tag{2}$$

Enthalpy and entropy values of MB were obtained from the slope of ($-\Delta H^\circ/R$) and intercept ($\Delta S^\circ/R$). The ΔG° was found to be −5.1 kJ mol^{-1} (Table 2) at 24°C, indicating a favorable adsorption process that was spontaneous and exothermic (ΔH°= −16.7 kJ mol^{-1}). The positive value of ΔS° (39.1 J mol^{-1} K^{-1}) suggests that there might be an affinity of the ACC toward MB. The exothermic nature was further confirmed by adsorption capacity (q_{max}) determinations, which showed that maximum adsorption of MB by ACC occurs at 24°C (298 K) followed by a decrease at warmer solution temperature (Fig. 6). MB, being more soluble at higher temperature will increase the desorption rate, thus resulting in MB being more difficult to be adsorbed. The same effect has also been previously reported where adsorption of MB decreases with the increase of temperature [28].

3.4. Adsorption isotherm and modeling

Adsorption isotherm was carried out using initial dye concentrations ranging from 0 to 1,000 mg L^{-1} (Fig. 7). Six different isotherm models (Eqs. (3)–(8)) *i.e.* the Langmuir [29], Freundlich [30], Temkin [31,32] Dubinin–Radushkevich (D–R) [32], Sips [33], and Redlich–Peterson (R–P) [34] models, together with five different error analyses (Eqs. (9)–(13)) [35], namely average relative error (ARE), sum square error (ERRSQ) [32], sum of absolute error (EABS), Hybrid fractional

Table 2
Thermodynamic parameters for adsorption of MB on ACC at different solution temperatures

T (K)	ΔG° (kJ mol^{-1})	ΔS° (J mol^{-1} K^{-1})	ΔH° (kJ mol^{-1})	q_{max} (mg g^{-1})
298	−5.05	39.12	−16.70	368.7
314	−4.31			273.7
324	−4.10			278.1
334	−3.78			271.8
344	−3.12			273.8

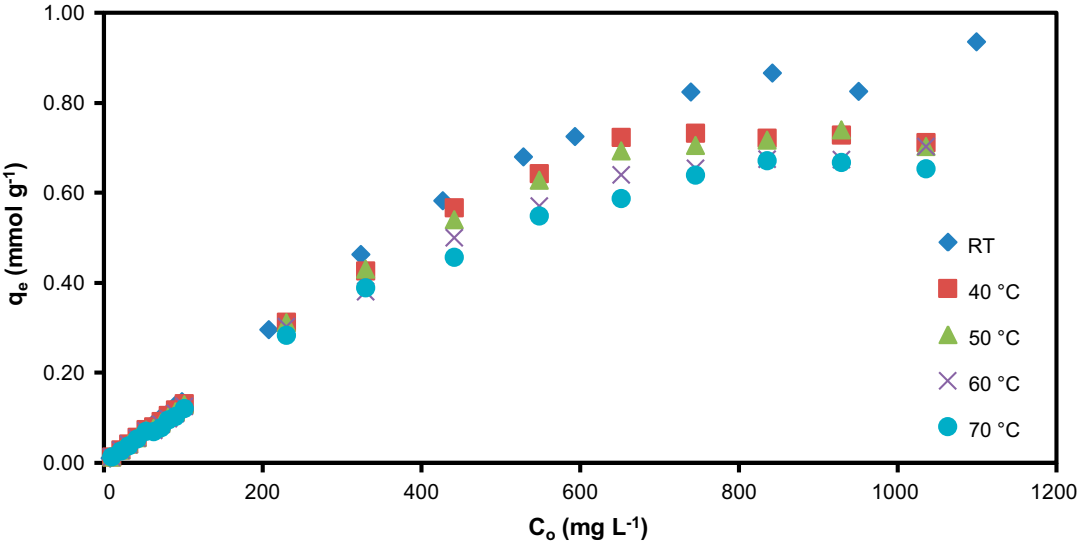

Fig. 6. Adsorption isotherms of MB on ACC at different temperatures.

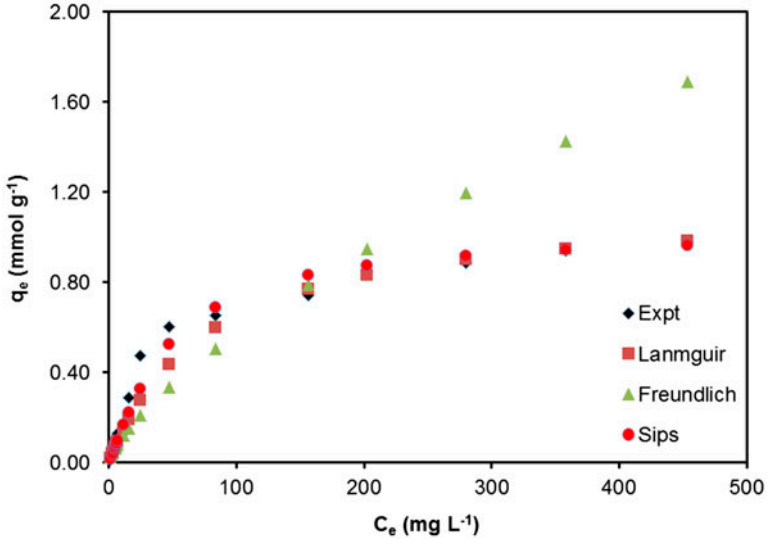

Fig. 7. Comparison of experimental and simulated adsorption isotherms of MB onto ACC.

error function (HYBRID), and the Marquardt's percent standard deviation (MPSD), were used to determine the best fit for the adsorption of MB on ACC.

Tables 3 and 4 show the parameters obtained for the six adsorption isotherm models and the five different error analyses, respectively. It can be seen that the R–P isotherm model, with the lowest linear coefficient R^2 (0.5911) and the highest errors, is the least fitting of all the models used. Hence its isotherm was omitted in Fig. 7.

$$\text{Langmuir isotherm:} \quad q_e = \frac{K_L q_{\max} C_e}{1 + K_L C_e} \tag{3}$$

$$\text{Freundlich isotherm:} \quad q_e = K_F C_e^{\frac{1}{n}} \tag{4}$$

$$\text{Temkin isotherm:} \quad q_e = \frac{RT}{b} \ln K_T C_e \tag{5}$$

$$\text{where } B = \frac{RT}{b}$$

$$\text{D} - \text{R isotherm:} \quad q_e = q_{\max} \exp(-\beta \varepsilon^2) \tag{6}$$

$$\varepsilon = RT \ \ln\left[1 + \frac{1}{C_e}\right]$$

$$E = \frac{1}{\sqrt{2\beta}}$$

Table 3
Parameters for different adsorption isotherm models

Isotherm Model	Parameters	Values
Langmuir	$q_{\max}$ (mmol g^{-1})	1.153
	K_L (L mmol^{-1})	0.0128
	R_L	0.0751
Freundlich	K_F (mmol g^{-1})	0.0212
	n	1.397
Temkin	K_T (L mmol^{-1})	0.3467
	b_T (J mol^{-1})	12,904
D–R	$q_{\max}$ (mmol g^{-1})	0.6211
	B (mmol^2 J^{-2})	1.10×10^{-6}
	E (J mol^{-1})	673.64
R–P	K_R (L g^{-1})	32
	g	0.2845
	a_R (L mmol^{-1})	1505.8
Sips	$q_{\max}$ (mmol g^{-1})	1.024
	K_L (L mmol^{-1})	0.0219

$$\text{R} - \text{P isotherm:} \quad q_e = \frac{K_R C_e}{1 + a_R C_e^g} \tag{7}$$

$$\text{Sips isotherm:} \quad q_e = \frac{q_{\max} K_s C_e^{\frac{1}{n}}}{1 + K_s C_e^{\frac{1}{n}}} \tag{8}$$

where q_e is the amount of dye adsorbed, C_e is the equilibrium concentration of the dye, $q_{\max}$ is the maximum adsorption capacity, K_F is the Freundlich constant, n is the empirical parameter which is related to the adsorption intensity, K_T is the equilibrium binding constant corresponding to the maximum binding energy, constant B is related to the heat of adsorption, T is absolute temperature, β gives the mean free energy, E of sorption per molecule of sorbate, K_s is Sips constant, $1/n$ is the Sips model exponent, K_R and a_R are the R-P constants, and g is the exponent which lies between 0 and 1.

$$\text{Average relative error (ARE):} \quad \frac{100}{n} \sum_{i=1}^{n} \left| \frac{q_{e,\text{meas}} - q_{e,\text{calc}}}{q_{e,\text{meas}}} \right|_i \tag{9}$$

$$\text{Sum squares error (ERRSQ):} \quad \sum_{i=1}^{n} (q_{e,\text{calc}} - q_{e,\text{meas}})_i^2 \tag{10}$$

$$\text{Sum of absolute error (EABS):} \quad \sum_{i=1}^{n} \left| q_{e,\text{meas}} - q_{e,\text{calc}} \right| \tag{11}$$

Hybrid fractional error function (HYBRID):

$$\frac{100}{n-p} \sum_{i=1}^{n} \left[\frac{(q_{e,\text{meas}} - q_{e,\text{calc}})^2}{q_{e,\text{meas}}} \right]_i \tag{12}$$

Marquardt's percent standard deviation (MPSD):

$$100 \sqrt{\frac{1}{n-p} \sum_{i}^{n} \left(\frac{q_{e,\text{meas}} - q_{e,\text{calc}}}{q_{e,\text{meas}}} \right)^2} \tag{13}$$

where $q_{e,\text{meas}}$ is the experimentally q_e value, $q_{e,\text{calc}}$ is the calculated q_e value, n is the number of parameters, and p is the number of data points.

Table 4
Error analyses on different isotherm models used for adsorption of MB on ACC

Isotherm model	R^2	ARE	ERRSQ	HYBRID	EABS	MPSD
Langmuir	0.9680	19.0	0.083	1.17	0.70	29.2
Freundlich	0.9014	36.8	1.036	7.76	2.62	51.3
Temkin	0.9708	121.3	0.071	10.21	0.85	383.3
D–R	0.9545	341.2	1.993	15.63	5.49	57.4
R–P	0.5911	81.2	4.774	19.89	6.75	91.8
Sips	0.9833	13.7	0.046	0.69	0.61	19.2

Of all the six isotherm models used, only the Langmuir and Sips isotherm models were best use to describe the adsorption of MB on ACC (Fig. 7). Both these models gave good R^2 of 0.9680 and 0.9833, respectively. The errors were low as compared to the other isotherm models. For example, both the Langmuir and Sips isotherms gave ARE values of < 20 as compared to the Freundlich, Temkin, D–R and R–P isotherm models whose ARE values are 36.8, 121.3, 341.2, and 81.2, respectively, clearly indicating that the latter four models are highly unsuitable to describe the adsorption process. The Langmuir isotherm model assumes a monolayer adsorption that takes place at specific homogenous sites, while the Sips model is a combination of both the Langmuir and Freundlich isotherm models. Overall, the Sips model, which is a combination of both the Langmuir and Freundlich models, gave a better fit with higher R^2 and lower errors as compared to the Langmuir model.

The adsorption isotherm of MB on ACC was carried out at ambient pH 6, which is higher than the pH_{pzc} of ACC. Under this experimental condition, deprotonation of the surface of ACC would result in the surface to be negatively charged. Further confirmation is obtained from the effect of medium pH, where an increase of adsorption capacity of ACC by 50% is observed from pH 2 to ambient pH. Increase in electrostatic force of attraction could be the reason for spontaneous and favorable adsorption observed in thermodynamics studies.

In this study, only conventional heating of ACC in an oven was used and no other pre-treatment procedures prior to adsorption were required. Many low-cost adsorbents having q_{max} values below 100 mg g^{-1} for the removal of MB had to be chemically treated and/or activated at high temperature or use microwave technology in order to enhance their adsorption capacity (Table 5). For example, bamboo powder had to be physiochemically activated with KOH and CO_2 and heated to a high temperature of 850˚C for its q_{max} to increase from 26.5 to 454 mg g^{-1}. As compared to some of these adsorbents, the adsorption capacity of untreated ACC with q_{max} 369 mg g^{-1} is far superior. Thus, ACC has a great potential to be used as a low-cost adsorbent for the removal of MB in wastewater treatment. There is also a possibility that this adsorption capacity could be further enhanced by activation of ACC through physiochemical means.

3.5. Kinetics of adsorption of MB on ACC

Kinetics studies of MB on ACC were determined using the pseudo-first-order [48], pseudo-second-order [49], and Weber–Morris intraparticle diffusion model [50] and their equations are shown in Table 6. Kinetics studies were carried out using 50 mg L^{-1} MB at ambient temperature. Fast adsorption of MB on ACC was observed with more than 50% of the dye was removed within 5 min (Fig. 8(a)). The kinetics parameters, obtained from its linear plots, showed that the pseudo-second-order model was the best fit model with R^2 = 0.9991 (Fig. 8(b)), compared to the pseudo-first-order model (R^2 = 0.7449). On the other hand, the $q_{e,calc}$ and $q_{e,exp}$ values of pseudo-second-order are 0.072 and 0.065 mmol g^{-1}, respectively, which are better than the pseudo-first-order (0.024 mmol g^{-1}). ACC shows a reasonably high rate constant (k_2) of 3.155 g $mmol^{-1}$ min^{-1} when compared to the other adsorbents [51].

3.6. FTIR of ACC

Fig. 9 shows adsorption of MB by ACC results in the broad OH and NH bands at 3,410 cm^{-1} to be shifted to 3,396 cm^{-1} indicating the binding of MB with hydroxyl and amino groups. In addition to ion exchange proposed, there is also evidence that carboxyl groups would also get involved in the binding with MB as seen from the significant shift for the strong C=O peak of carboxylic acid from 1,635 to 1,602 cm^{-1}. At ambient pH (>pH_{pzc}) in which the adsorption was carried out, the COOH groups will be deprotonated to form COO^- carboxylate ions. Hence there would be attraction between the cationic MB

Table 5
Comparison of maximum adsorption capacity for the removal of MB on selected adsorbents

Adsorbent		q_{max} (mg g^{-1})	Reference
Artocarpus camansi core		369	This work
Artocarpus hetorophyllus peel	Untreated	286	[8]
	Microwave induced NaOH activated	400	[7]
Artocarpus camansi peel		409	[18]
Artocarpus odoratissimus peel		185	[16]
Milled sugarcane bagasse		31	[36]
Cupressus sempervirens cones	Untreated	198	[37]
	Alkaline treated	218	[38]
Graphene		154	[39]
Potato stem		42	[40]
Grape pulp		79	[41]
Eichhornia charcoal		22	[42]
Brazilian pine fruit shell	Untreated	185	[43]
	Acid treated	143	
Bamboo charcoal	Non activated	27	[44]
	KOH & CO_2 treated & heat at 850°C	454	[45]
Acid modified kenaf core fiber		132	[46]
Peat	Untreated	144	[23]
Cotton stalk	Untreated	147	[47]
	Phosphoric acid treated	222	

Table 6
Kinetics models used for the adsorption of MB onto ACC

Kinetics model	Non linear	Linear	Plot
Pseudo-first-order	$\frac{dq_t}{dt} = k_1(q_e - q_t)$	$\log(q_e - q_t) = \log(q_e) - \frac{k_t}{2.303}$	$\log(q_e - q_t)$vs t
Pseudo-second-order	$\frac{dq}{dt} = k_2(q_e - q_t)^2$	$\frac{t}{q_t} = \frac{1}{k_2 q_e^2} + \frac{1}{q_e}t$	$\frac{t}{q_t}$vs t
Intraparticle diffusion	$q_t = K_3 t^{1/2}$	$q_t = K_3 t^{1/2} + C$	q_t vs $t^{1/2}$

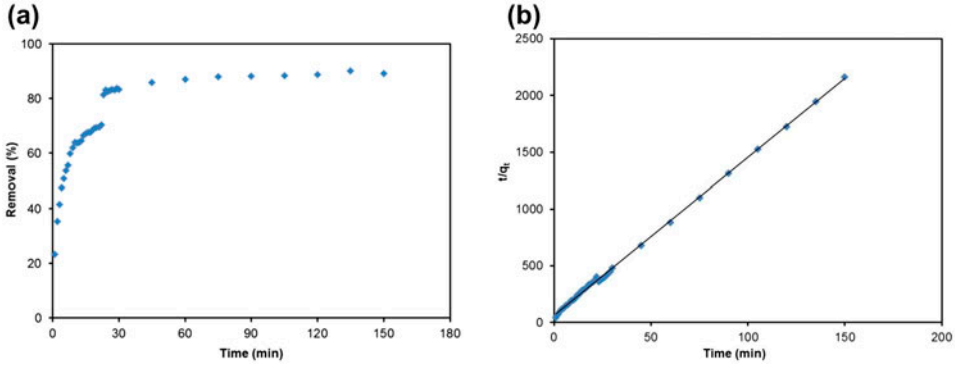

Fig. 8. (a) Kinetics studies of MB on ACC and (b) pseudo-second-order kinetic plot.

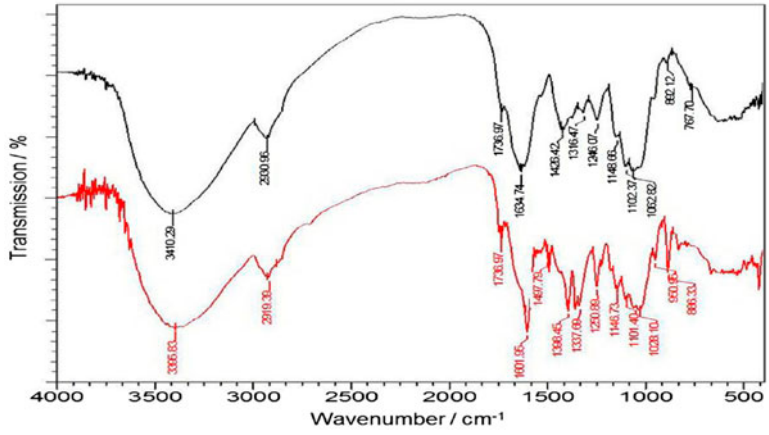

Fig. 9. FTIR spectra of ACC before (top) and after (bottom) treatment with MB.

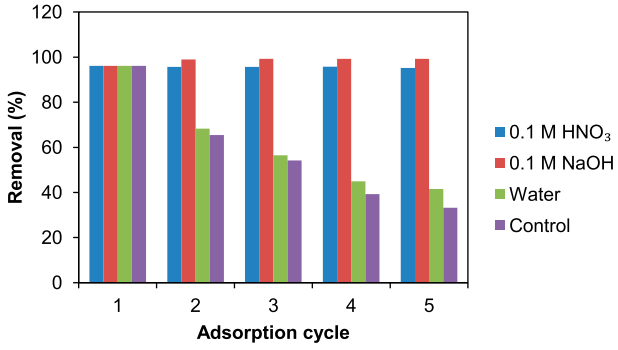

Fig. 10. Regeneration of ACC showing removal efficiency of MB for five consecutive cycles.

and the carboxylate ions. Thus, functional groups, such as OH, NH, and C=O, on the surface of the ACC provide potential active sites and are involved in sorption process with MB.

3.7. Regeneration of ACC

After adsorption of MB on ACC, regeneration studies were attempted with 0.1 M HNO_3, 0.1 M NaOH, and distilled water (Fig. 10). It was determined that both acid treatment and base treatment were able to desorb already adsorbed MB as compared to distilled water, regenerating the adsorbent, which thereafter shows adsorption properties as of initially. However, treatment with distilled water is not favorable in desorbing MB. This concludes that MB would not be removed back to the environment significantly under normal atmospheric conditions, such as rain events. Disposal of MB-adsorbed adsorbent would not immediately pose an environmental threat.

4. Conclusions

It is concluded that the core of *Artocarpus camansi* is an effective low-cost adsorbent for the removal of MB dye with high maximum adsorption capacity as compared to many reported low-cost adsorbents. Thermodynamics studies indicate favorable and spontaneous adsorption with the maximum adsorption capacity at 298 K. The adsorption isotherm, corresponding to the Langmuir and Sips models, gave far superior adsorption capacities (q_{max}) to most adsorbents. Unlike for other adsorbents which had to be activated to enhance adsorption capacity, ACC requires no pre-treatment of sample, except for oven-drying. This is an advantage in real life application. Adsorption of MB dye on ACC follows pseudo-second-order kinetics with relative high rate constants. Fast kinetics coupled with high q_{max} make ACC a potentially attractive low-cost adsorbent in wastewater treatment. Treatment of real industrial effluent containing MB is the next logical step of this research.

Acknowledgments

The authors would like to thank the Government of Negara Brunei Darussalam and the Universiti Brunei Darussalam (UBD) for their financial support in carrying out this research. The authors are also grateful to the Biology Department and CAMES at UBD for the use of SEM and XRF.

References

[1] V.K. Gupta, Suhas, Application of low-cost adsorbents for dye removal—A review, J. Environ. Manage. 90 (2009) 2313–2342.
[2] L.B.L. Lim, N. Priyantha, U.K. Ramli, H.I. Chieng, Adsorption of Cd(II) ions using Lamiding, a wild vegetable from Brunei Darussalam, J. Appl. Phytechnol. Environ. Sanitat. 3 (2013) 65–74.

[3] L.B.L. Lim, N. Priyantha, D.T.B. Tennakoon, H.I. Chieng, C. Bandara, Sorption characteristics of peat of Brunei Darussalam I: Characterization of peat and adsorption equilibrium studies of methylene blue—Peat interactions, Cey. J. Sci. (Phy. Sci.) 17 (2013) 41–51.
[4] H.I. Chieng, L.B.L. Lim, N. Priyantha, Adsorption of copper(II) ions by peat from pristine and disturbed sites: Equilibrium, thermodynamics and kinetics study, J. Appl. Sci. Environ. Sanitat. 8 (2013) 303–312.
[5] L.B.L. Lim, H.I. Chieng, F.L. Wimmer, The nutrient composition of *Artocarpus champeden* and its hybrid (*Nanchem*) in Negara Brunei Darussalam, ASEAN J. Sci. Technol. Dev. 28 (2011) 122–138.
[6] Y.P. Tang, B.L.L. Linda, L.W. Franz, Proximate analysis of *Artocarpus odoratissimus* (Tarap) in Brunei Darussalam, Int. Food Res. J. 20 (2013) 409–415.
[7] K.Y. Foo, B.H. Hameed, Potential of jackfruit peel as precursor for activated carbon prepared by microwave induced NaOH activation, Bioresour. Technol. 112 (2012) 143–150.
[8] B.H. Hameed, Removal of cationic dye from aqueous solution using jackfruit peel as non-conventional low-cost adsorbent, J. Hazard. Mater. 162 (2009) 344–350.
[9] B.S. Inbaraj, N. Sulochana, Use of jackfruit peel carbon (JPC) for adsorption of rhodamine-B, a basic dye from aqueous solution, Indian J. Chem. Technol. 13 (2006) 17–23.
[10] M. Jayarajan, R. Arunachalam, G. Annadurai, Agricultural wastes of jackfruit peel nano-porous adsorbent for removal of rhodamine dye, Asian J. Appl. Sci. 4 (2011) 263–270.
[11] B.S. Inbaraj, N. Sulochana, Carbonised jackfruit peel as an adsorbent for the removal of Cd(II) from aqueous solution, Bioresour. Technol. 94 (2004) 49–52.
[12] P.D. Saha, S. Chakraborty, S. Chowdhury, Batch and continuous (fixed-bed column) biosorption of crystal violet by *Artocarpus heterophyllus* (jackfruit) leaf powder, Colloids Surf., B 92 (2012) 262–270.
[13] M.T. Uddin, M. Rukanuzzaman, M.M.R. Khan, M.A. Islam, Jackfruit (*Artocarpus heterophyllus*) leaf powder: An effective adsorbent for removal of methylene blue from aqueous solution, Indian J. Chem. Technol. 16 (2009) 142–149.
[14] L.B.L. Lim, N. Priyantha, D.T.B. Tennakoon, M.K. Dahri, Biosorption of cadmium(II) and copper(II) ions from aqueous solution by core of *Artocarpus odoratissimus*, Environ. Sci. Pollut. Res. 19 (2012) 3250–3256.
[15] N. Priyantha, L.B.L. Lim, D.T.B. Tennakoon, N.H.M. Mansor, M.K. Dahri, H.I. Chieng, Breadfruit (Artocarpus altilis) waste for bioremediation of Cu(II) and Cd (II) ions from aqueous medium, Cey. J. Sci. (Phy. Sci.) 17 (2013) 19–29.
[16] L.B.L. Lim, N. Priyantha, H.I. Chieng, M.K. Dahri, D.T.B. Tennakoon, T. Zehra, M. Suklueng, *Artocarpus odoratissimus* skin as a potential low-cost biosorbent for the removal of methylene blue and methyl violet 2B, Desalin. Water Treat. (2013) 1–12, doi:10.1080/19443994.2013.852136.
[17] L.B.L. Lim, N. Priyantha, N.H.M. Mansor, *Artocarpus altilis* (breadfruit) skin as a potential low-cost biosorbent for the removal of crystal violet dye: Equilibrium, thermodynamics and kinetics studies, Environ. Earth Sci. (2014) doi:10.1007/s12665-014-3616-8.
[18] L.B.L. Lim, N. Priyantha, D.T.B. Tennakoon, H.I. Chieng, M.K. Dahri, M. Suklueng, Breadnut peel as a highly effective low-cost biosorbent for methylene blue: Equilibrium, thermodynamics and kinetic studies, Arab. J. Chem. (2014), doi:10.1016/j.arabjc.2013.12.018.
[19] H.I. Chieng, L.B.L. Lim, N. Priyantha, Enhancing adsorption capacity of toxic malachite green dye through chemically modified breadnut peel: Equilibrium, thermodynamics, kinetics and regeneration studies, Environ. Technol. 36 (2015) 86–97. doi:10.1080/09593330.2014.938124.
[20] A. Ghali, M. Baouab, M. Roudesli, Use of amino-modified cotton fibers loaded with copper ions for anionic dye removal under batch and fixed-bed systems: A comparative study, Fibers Polym. 14 (2013) 65–75.
[21] V.K. Gupta, S. Agarwal, P. Singh, D. Pathania, Acrylic acid grafted cellulosic *Luffa cylindrical* fiber for the removal of dye and metal ions, Carbohyd. Polym. 98 (2013) 1214–1221.
[22] M.C. Ncibi, B. Mahjoub, M. Seffen, Adsorptive removal of textile reactive dye using *Posidonia oceanica* (L.) fibrous biomass, Int. J. Environ. Sci. Technol. 4 (2007) 433–440.
[23] H.I. Chieng, T. Zehra, L.L. Lim, N. Priyantha, D.T.B. Tennakoon, Sorption characteristics of peat of Brunei Darussalam IV: Equilibrium, thermodynamics and kinetics of adsorption of methylene blue and malachite green dyes from aqueous solution, Environ. Earth Sci. 72 (2014) 2263–2277.
[24] K. Raj, A. Kardam, J. Arora, S. Srivastava, M.M. Srivastava, Adsorption behavior of dyes from aqueous solution using agricultural waste: Modeling approach, Clean Technol. Environ. Policy 15 (2013) 73–80.
[25] E. Eren, A. Tabak, B. Eren, Performance of magnesium oxide-coated bentonite in removal process of copper ions from aqueous solution, Desalination 257 (2010) 163–169.
[26] R. Liu, B. Zhang, D. Mei, H. Zhang, J. Liu, Adsorption of methyl violet from aqueous solution by halloysite nanotubes, Desalination 268 (2011) 111–116.
[27] R. Aravindhan, J.R. Rao, B.U. Nair, Removal of basic yellow dye from aqueous solution by sorption on green alga *Caulerpa scalpelliformis*, J. Hazard. Mater. 142 (2007) 68–76.
[28] X. Han, W. Wang, X. Ma, Adsorption characteristics of methylene blue onto low cost biomass material lotus leaf, Chem. Eng. J. 171 (2011) 1–8.
[29] I. Langmuir, The constitution and fundamental properties of solids and liquids. Part I. Solids, J. Am. Chem. Soc. 38 (1916) 2221–2295.
[30] H.M.F. Freundlich, Uber die adsorption in losungen (adsorption in solution), Z. Phys. Chem. 57 (1906) 384–470.
[31] M.I. Temkin, V. Pyzhev, Kinetics of ammonia synthesis on promoted iron catalyst, Acta. Phys. Chim. URSS 12 (1940) 327–356.
[32] M.M. Dubinin, L.V. Radushkevich, The equation of the characteristic curve of the activated charcoal, Proc. Acad. Sci. USSR Phys. Chem. Sec. 55 (1947) 331–337.
[33] R. Sips, Combined form of Langmuir and Freundlich equations, J. Chem. Phys. 16 (1948) 490–495.

[34] O. Redlich, D.L. Peterson, A useful Adsorption Isotherm, J. Phys. Chem. 63 (1959) 1024–1029.
[35] G. Frédéric, N. Morin-Crini, R. François, P.-M. Badot, C. Grégorio, Adsorption isotherm models for dye removal by cationized starch-based material in a single component system: Error analysis, J. Hazard. Mater. 157 (2008) 34–46.
[36] Z. Zhang, I.M. O'Hara, G.A. Kent, W.O.S. Doherty, Comparative study on adsorption of two cationic dyes by milled sugarcane bagasse, Ind. Crop. Prod. 42 (2013) 41–49.
[37] M.E. Fernandez, G.V. Nunell, P.R. Bonelli, A.L. Cukierman, Effectiveness of *Cupressus sempervirens* cones as biosorbent for the removal of basic dyes from aqueous solutions in batch and dynamic modes, Bioresour. Technol. 101 (2010) 9500–9507.
[38] M.E. Fernandez, G.V. Nunell, P.R. Bonelli, A.L. Cukierman, Batch and dynamic biosorption of basic dyes from binary solutions by alkaline-treated cypress cone chips, Bioresour. Technol. 106 (2012) 55–62.
[39] T. Liu, Y. Li, Q. Du, J. Sun, Y. Jiao, G. Yang, Z. Wang, Y. Xia, W. Zhang, K. Wang, H. Zhu, D. Wu, Adsorption of methylene blue from aqueous solution by graphene, Colloids Surf., B 90 (2012) 197–203.
[40] N. Gupta, A.K. Kushwaha, M.C. Chattopadhyaya, Application of potato (*Solanum tuberosum*) plant wastes for the removal of methylene blue and malachite green dye from aqueous solution, Arab. J. Chem. (2011) doi:10.1016/j.arabjc.2011.07.021.
[41] H. Saygili, G.A. Saygili, F. Güzel, Using grape pulp as a new alternative biosorbent for removal of a model basic dye, Asia-Pac. J. Chem. Eng. 9 (2013) 214–225.
[42] Sumanjit, S. Rani, R.K. Mahajan, Equilibrium, kinetics and thermodynamics parameters for adsorptive removal of dye Basic Blue 9 by ground nut shells and Eichhornia, Arab. J. Chem. (2012) doi: http://dx.doi.org/10.1016/j.arabjc.2012.03.013.
[43] B. Royer, N.F. Cardoso, E.C. Lima, J.C.P. Vaghetti, N.M. Simon, T. Calvete, R.C. Veses, Applications of Brazilian pine-fruit shell in natural and carbonized forms as adsorbents to removal of methylene blue from aqueous solutions—Kinetic and equilibrium study, J. Hazard. Mater. 164 (2009) 1213–1222.
[44] P. Liao, I.Z. Malik, W. Zhang, S. Yuan, M. Tong, K. Wang, J. Bao, Adsorption of dyes from aqueous solutions by microwave modified bamboo charcoal, Chem. Eng. J. 195–196 (2012) 339–346.
[45] B.H. Hameed, A.T.M. Din, A.L. Ahmad, Adsorption of methylene blue onto bamboo-based activated carbon: Kinetics and equilibrium studies, J. Hazard. Mater. 141 (2007) 819–825.
[46] M.S. Sajab, C.H. Chia, S. Zakaria, S.M. Jani, M.K. Ayob, K.L. Chee, P.S. Khiew, W.S. Chiu, Citric acid modified kenaf core fibres for removal of methylene blue from aqueous solution, Bioresour. Technol. 102 (2011) 7237–7243.
[47] H. Deng, J. Lu, G. Li, G. Zhang, X. Wang, Adsorption of methylene blue on adsorbent materials produced from cotton stalk, Chem. Eng. J. 172 (2011) 326–334.
[48] S. Lagergren, Zur theorie der sogenannten adsorption geloster stoffe (About the theory of so-called adsorption of soluble substances), Academy of Sciences, Royal Swedish, 24 (1898) 1–39.
[49] Y.S. Ho, G. McKay, Sorption of dye from aqueous solution by peat, Chem. Eng. J. 70 (1998) 115–124.
[50] W.J. Weber, J.C. Morris, Kinetics of adsorption on carbon from solution, J. Sanitary Eng. Div. Am. Soc. Civil. Eng. 89 (1963) 31–60.
[51] P. Li, Y.J. Su, Y. Wang, B. Liu, L.M. Sun, Bioadsorption of methyl violet from aqueous solution onto Pu-erh tea powder, J. Hazard. Mater. 179 (2010) 43–48.